Acta Cryst E CRYSTALLOGRAPHIC COMMUNICATIONS

ISSN 2056-9890

Synthesis, crystal structure and Hirshfeld surface analysis of phenylmethanaminium 2-oxo-2*H*-chromene-3-carboxylate

M. Sunithakumari,[a] M.U. Gagan,[b] V. Dwarakanath,[b] H.T. Srinivasa,[c] H. C. Devarajegowda[a] and B. S. Palakshamurthy[d]*

[a]Department of Physics, Yuvaraja's College, University of Mysore, Mysore 570005, Karnataka, India, [b]Department of Biotechnology, U.C.S, Tumkur University, Tumkur, Karnataka-572103, India, [c]Raman Research Institute, C. V. Raman, Avenue, Sadashivanagar, Bangalore-560080, Karnataka, India, and [d]Department of PG Studies and Research in Physics, Albert Einstein Block, UCS, Tumkur University, Tumkur, Karnataka-572103, India. *Correspondence e-mail: palaksha.bspm@gmail.com

Received 16 March 2026
Accepted 31 March 2026

Edited by L. Van Meervelt, Katholieke Universiteit Leuven, Belgium

Keywords: crystal structure; co-crystals; Hirshfeld surface; 2-oxo-2*H*-chromene; benzyl amine.

CCDC reference: 2542776

Supporting information: this article has supporting information at journals.iucr.org/e

The title salt, $C_7H_{10}N^+\cdot C_{10}H_4O^-$, formed between 2-oxo-2*H*-chromene-3-carboxylic acid and benzylamine crystallizes in the triclinic space group $P\overline{1}$. Proton transfer from 2-oxo-2*H*-chromene-3-carboxylic acid to the NH_2 group of benzylamine results in a N—H···(O,O) hydrogen bond between cation and the carboxylate group of the anion. The 2-oxo-2*H*-chromene moiety is almost planar with a dihedral angle between the two fused rings of 1.48 (11)°. The dihedral angle between the rings of the anion and cation is 29.49 (10)°. In the crystal, N—H···O hydrogen-bonding interactions generate an $R_4^4(12)$ synthon parallel to the *ac* plane. The molecules are linked by further C—H···π interactions, which consolidate the packing. In addition, π–π stacking interactions are observed with centroid-to-centroid distances of 3.5832 (14) and 3.8167 (15) Å. The two-dimensional fingerprint plots indicates that the most important contributions to the crystal packing are from H···H (39.7%), H···O/O···H (30.6%) and H···C/C···H (20.9%) contacts. The antibacterial activity, with MIC values of 30 µg ml^{-1} against *S. aureus* and 25 µg ml^{-1} against *E. coli*. The lower MIC against *E. coli* suggests that the compound is more effective against Gram-negative bacteria than Gram-positive bacteria.

1. Chemical context

Chromene and coumarin derivatives possess considerable pharmacological relevance. 2*H*-Chromene oxime derivatives exhibit antiproliferative activity against A549, MCF-7 and MDA-MB-231 cell lines (Bandaru *et al.*, 2025), while coumarin-3-carboxamides demonstrate both antibacterial and anticancer properties (Phutdhawong *et al.*, 2021). Similarly, 2-oxo-2*H*-chromene-3-carboxylates show cytotoxicity toward HepG2, HeLa and HCT116 tumour cell lines (Ji *et al.*, 2021), and related chromene-3-carboxylates display activity against both Gram-positive and Gram-negative bacteria (Venugopala *et al.*, 2013). Coumarins are also known inhibitors of cyclooxygenase and lipoxygenase pathways (Stefanachi *et al.*, 2018). Furthermore, chromene derivatives constitute validated pharmacophores in anticoagulant therapy; clinically used agents inhibit vitamin K epoxide reductase, thereby suppressing vitamin K-dependent clotting factors (Ansell, 2008).

Beyond pharmaceutical applications, functionalized phenylmethanaminium iodide salts have been investigated as surface-passivation agents in perovskite solar cells, improving device efficiency and operational stability (Yasa *et al.*, 2025). Phenylmethanaminium (benzylammonium) derivatives additionally exhibit diverse biological activities, including anti-

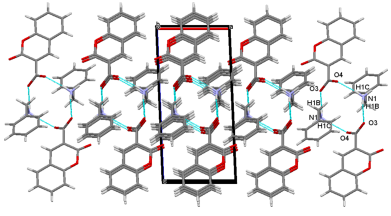

OPEN ACCESS
Published under a CC BY 4.0 licence

tumor (Kemnitzer *et al.*, 2004), antibacterial (Ganapathi *et al.*, 2025) and anti-inflammatory effects (Cacabelos *et al.*, 2024). Collectively, these findings highlight the structural versatility and biological significance of chromene and phenylmethanaminium frameworks and support their continued investigation in crystal engineering and pharmaceutical materials research. s part of our studies in this area, we now report the synthesis and structure of the title salt $C_7H_{10}N^+\cdot C_{10}H_4O^-$, (I).

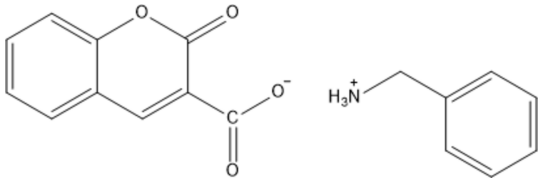

2. Structural commentary

The molecular structure of (I) is shown in Fig. 1. The dihedral angle between the rings of the almost planar (r.m.s. deviation = 0.015 Å) fused ten-membered 2-oxo-2*H*-chromene moiety is 1.48 (11)° whereas the dihedral angle between 2-oxo-2*H*-chromene and the aromatic ring of benzylamine is 29.49 (10)° for the species in the asymmetric unit. Proton transfer from the 2-oxo-2*H*-chromene-3-carboxylic acid to the NH_2 substituent of ethylbenzene lead to the formation of the title salt with a strong N1—H1*A*···O3 hydrogen bond (Table 1). The torsion angles C2—C1—C10—O3 and N1—C17—C11—C16 are 44.9 (3) and 78.0 (3)°, respectively. The angle made by the atoms C11—C17—N1 is 113.3 (2)°.

3. Supramolecular features

In the crystal, the ions are linked by weak N1—H1*A*···O2 and stronger N1—H1*A*···O3 hydrogen bonds (Table 1). A set of

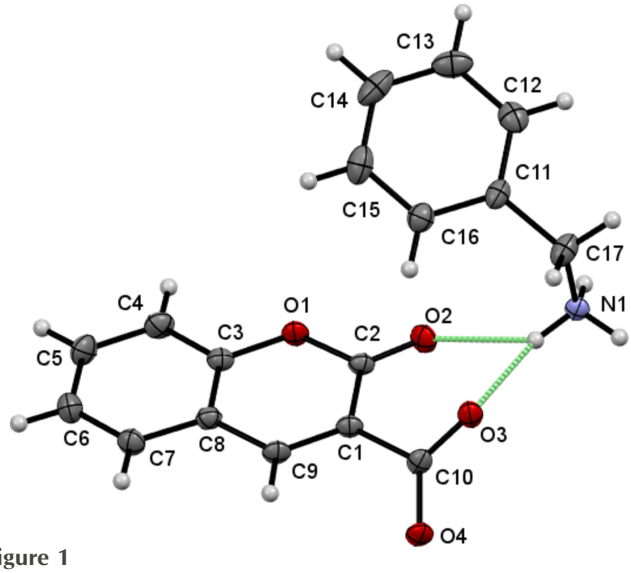

Figure 1
The title salt with atom-numbering scheme and 50% probability ellipsoids. Dashed lines represent hydrogen bonds.

Table 1
Hydrogen-bond geometry (Å, °).

*Cg*4 is the centroid of the C11–C16 ring.

D—H···*A*	*D*—H	H···*A*	*D*···*A*	*D*—H···*A*
N1—H1*A*···O2	0.89	2.40	3.068 (3)	132
N1—H1*A*···O3	0.89	1.99	2.752 (3)	142
N1—H1*B*···O3^{i}	0.89	1.94	2.791 (3)	158
N1—H1*C*···O4^{ii}	0.89	1.83	2.716 (3)	174
C17—H17*B*···*Cg*4^{iii}	0.97	2.76	3.613 (3)	147

Symmetry codes: (i) $-x, -y+1, -z+1$; (ii) $x-1, y, z$; (iii) $-x, -y, -z+1$.

2-oxo-2*H*-chromene-3-carboxylate phenylmethanaminium molecules generate a layered two-dimensional supramolecular architecture propagating in the *ac* plane as shown in Fig. 2. The tetramer (two cations and two anions) of molecules generate an $R_4^4(12)$ synthon. Two nitrogen donor atoms, one from each phenylmethanaminium cation and four oxygen acceptor atoms, two from each 2-oxo-2*H*-chromene-3-carboxylate cation, are involved in the synthon. The molecules are linked by C17—H17*B*···*Cg*4 interactions (*Cg*4 is the centroid of the C11–C16 ring; Fig. 3). The crystal packing is further consolidated by π–π stacking interactions with centroid-to-centroid distances $Cg1\cdots Cg2^{i}$ = 3.5832 (14) Å and

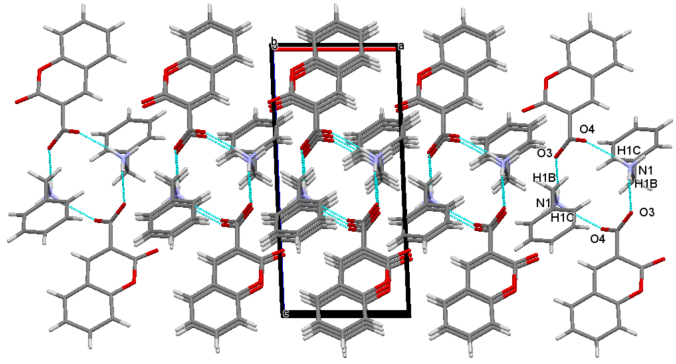

Figure 2
Packing diagram with N—H···O hydrogen bonds shown as blue dashed lines.

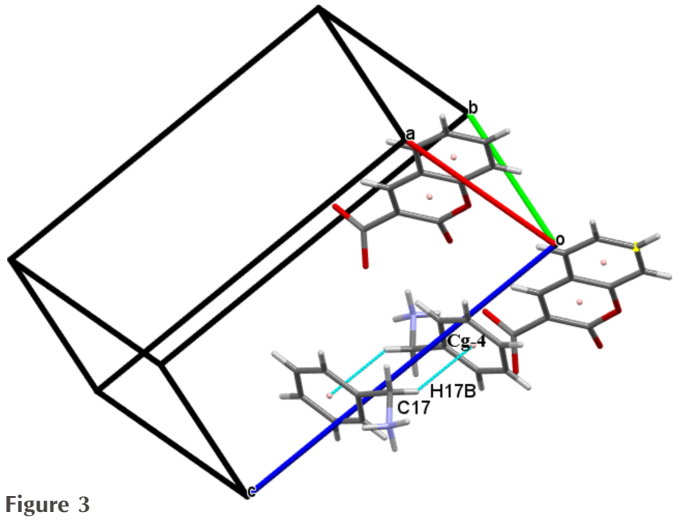

Figure 3
Partial packing diagram with C—H···π interactions shown as blue dashed lines.

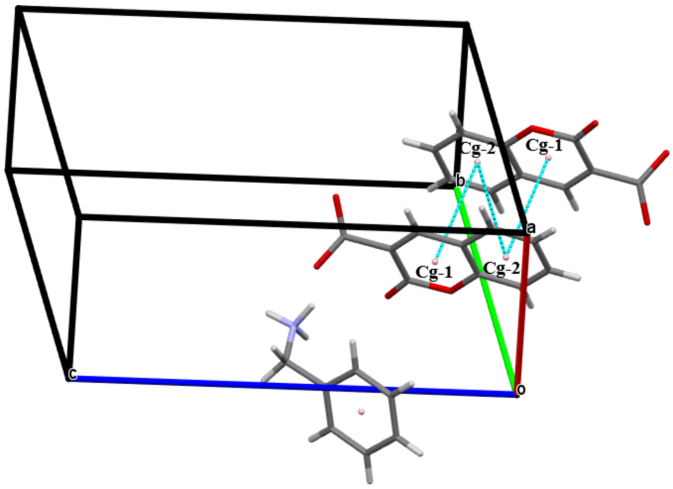

Figure 4
The molecular packing of (I) with $\pi\cdots\pi$ stacking interactions shown as blue dashed lines.

*Cg*2$\cdots$*Cg*2^{i} = 3.8167 (15) Å [slippage = 1.675 Å; symmetry code: (i) $1-x, 1-y, -z'$; *Cg*1 and *Cg*2 are the centroids of the O1/C2/C1/C9/C8/C3 and C3–C8 rings, respectively; Fig. 4].

4. Database survey

A search of the Cambridge Structural Database (CSD, version 5.42, November 2020 update; Groom *et al.*, 2016) for compounds containing a 2-oxo-2*H*-chromene-3-carboxylate moiety yielded over thirty entries. Among these, butane-1,4-diammonium bis(2-oxo-2*H*-chromene-3-carboxylate) CSD (refcode GEPLUK; Das *et al.*, 2012), 4-(3,4-dichlorophenyl)-*N*-methyl-1,2,3,4-tetrahydronaphthalen-1-aminium 2-oxo-2*H*-chromene-3-carboxylate (VAHHEU; Escudero *et al.*, 2016), and 2,6-diaminopyridinium 2-oxo-2*H*-chromene-3-carboxylate (VAXRIX; Yan *et al.*, 2012) bear similar 2-oxo-2*H*-chromene substituents and exhibit a dihedral angle between both rings of the ten-membered 2-oxo-2*H*-chromene moiety of 1.86, 1.96, and 0.44°, respectively, comparable to the title compound [1.48 (11)°].

Furthermore, a search for phenylmethanaminium fragments also yielded over thirty entries. Among these, three structures are comparable to the title salt: phenylmethanaminium naphthalene-2-sulfonate (DOXLEK01; Chakraborty *et al.*, 2020), dodecakis(phenylmethanaminium) tris(benzene-1,2,4,5-tetracarboxylate) octahydrate (EZOCUU; Ye *et al.*, 2021), and phenylmethanaminium 4-(2,4,6-triisopropylbenzoyl) benzoate (CARGIM01; Bąkowicz *et al.*, 2014). In these structures, the C(ring)—C—N angle is 112.0, 114.8, and 113.5°, comparable to 113.3 (2)° for the title salt.

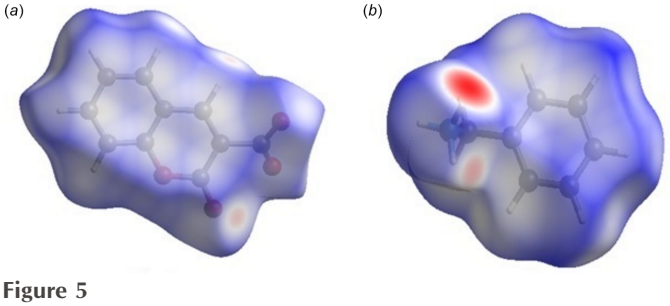

Figure 5
View of the three-dimensional Hirshfeld surface of the 2-oxo-2*H*-chromene-3-carboxylate moiety (*a*) and the phenylmethanaminium fragment (*b*) plotted over d_{norm}.

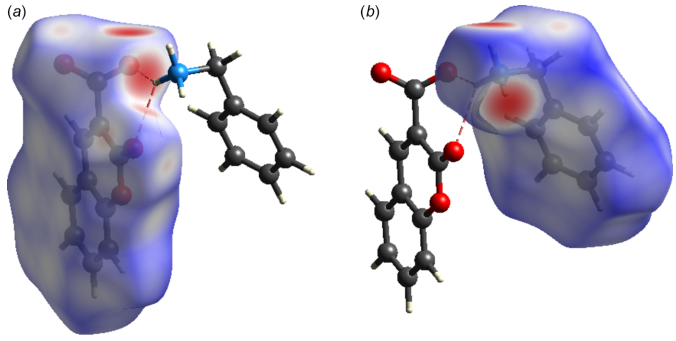

Figure 6
Hirshfeld surface of (I) plotted over d_{norm} with the N—H$\cdots$O interactions near the red spots shown for the 2-oxo-2*H*-chromene-3-carboxylate moiety (*a*) and the phenylmethanaminium fragment (*b*)

5. Hirshfeld surface analysis

A Hirshfeld surface analysis (Hirshfeld, 1977; Spackman & Jayatilaka, 2009) was carried out using *Crystal Explorer 17.5* (Spackman *et al.*, 2021) to further quantify the intermolecular interactions listed Table 1. The three-dimensional Hirshfeld surfaces plotted over d_{norm} separately for the 2-oxo-2*H*-chromene-3-carboxylate moiety (*a*) and the phenylmethanaminium fragment (*b*) are shown in Fig. 5. For both components of the salt, the intermolecular interactions near the red spots are presented in Fig. 6. The two-dimensional fingerprint plots generated separately for the 2-oxo-2*H*-chromene-3-carboxylate moiety (Fig. 7) and phenylmethanaminium fragment (Fig. 8), show contributions from

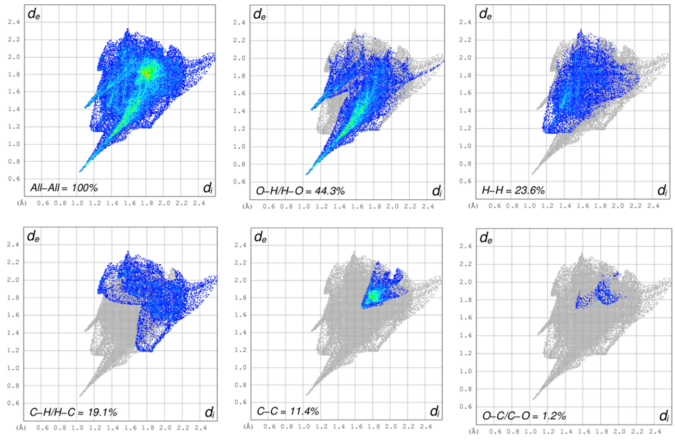

Figure 7
The two-dimensional fingerprint plots for the 2-oxo-2*H*-chromene-3-carboxylate moiety, showing all interactions, and delineated into O$\cdots$H/H$\cdots$O (44.3%), H$\cdots$H (23.6%), H$\cdots$C/C$\cdots$H (19.1%), C$\cdots$C (11.4%), and O$\cdots$C/C$\cdots$O (1.2%) contacts.

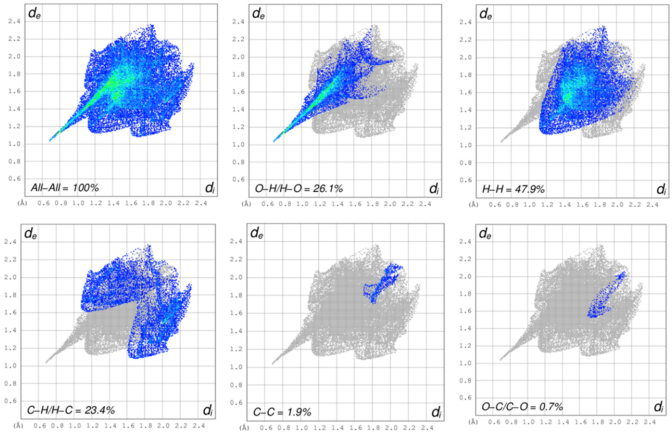

Figure 8
The two-dimensional fingerprint plots for the phenylmethanaminium moiety, showing all interactions, and delineated into O···H/H···O (26.1%), H···H (47.9%), H···C/C···H (23.4%), C···C (1.9%), and O···C/C···O (0.7%) contacts.

O···H/H···O, H···H, H···C/C···H, C···C, and O···C/C···O contacts of 44.3%, 23.6%, 19.1%, 11.4% and 1.2%, respectively, for the 2-oxo-2*H*-chromene-3-carboxylate moiety, whereas 26.1%, 47.9%, 23.4%, 1.9% and 0.7%, respectively, for the phenylmethanaminium fragment. Fig. 9*a* illustrates the Hirshfeld surface plotted over d_{norm} generated simultaneously for both fragments. The intermolecular interactions present near the red spots are visualized in Fig. 9*b*. The 2D finger plot for the combined fragments (Fig. 9*c*) shows two sharp spikes at $d_i + d_e \simeq 1.7$ Å resulting from O···H/H···O interactions with a contribution of 30.6% (Fig. 9*d*).

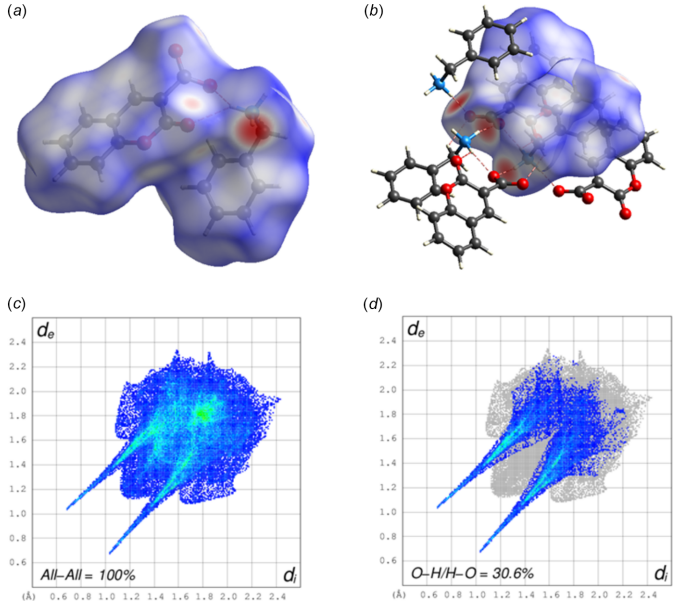

Figure 9
View of the Hirshfeld surface of (I) plotted over d_{norm} (*a*), the Hirshfeld surface with the N—H···O intermolecular interactions (*b*),, two-dimensional fingerprint plots for the entire salt (*c*) and two-dimensional fingerprint plots showing sharp O···H/H···O spikes (30.6%) (*d*).

6. Antibacterial activity studies

The antibacterial activity of the title salt was evaluated by the agar disc-diffusion method following standard bioassay procedures (Atta-ur-Rahman *et al.*, 2001) and antimicrobial susceptibility testing guidelines recommended by the clinical and laboratory standards institute (Pierce *et al.*, 2023). The test organisms employed were *Staphylococcus aureus* (Gram-positive) and *Escherichia coli* (Gram-negative). The standard antibacterial drug ciprofloxacin was used as the reference control. The salt was dissolved in dimethyl sulfoxide (DMSO) to prepare a stock solution (1mg mL^{-1}). Serial dilutions were prepared to obtain concentrations of 100, 75, 50, 40, 35, 30, 25, 20, 15, and 12.5 µg mL^{-1}. A solvent control containing only DMSO was tested under identical experimental conditions to ensure that the solvent had no inhibitory effect on bacterial growth; no zone of inhibition was observed. Sterile filter paper discs (6 mm diameter) were impregnated with 10 µL of each test solution and dried under aseptic conditions. The discs were placed on Mueller–Hinton agar plates previously inoculated with standardized bacterial suspensions ($\sim 10^8$ CFU mL^{-1}; CFU = colony forming unit). The plates were incubated at 37 °C for 16–18 h. After incubation, the zones of inhibition were measured in millimetres (mm). The minimum inhibitory concentration (MIC) was determined as the lowest concentration showing visible inhibition of bacterial growth. The percentage inhibition of the title salt was calculated relative to the standard drug ciprofloxacin, whose inhibition zone was considered as 100%. The standard drug ciprofloxacin shows MIC values of 15 µg mL^{-1} against *S. aureus* and 15 µg mL^{-1} against *E. coli*. The title salt exhibited moderate antibacterial activity, with MIC values of 30 µg mL^{-1} against *S. aureus* and 25 µg mL^{-1} against *E. coli*, The slightly lower MIC against *E. coli* suggests that the title salt is marginally more effective against Gram-negative bacteria than Gram-positive bacteria.

7. Synthesis and crystallization

The title salt was prepared by dissolving 2-oxo-2*H*-chromene-3-carboxylic acid and phenylmethanamine in a 1:1 molar ratio in a small excess of ethanol. The mixture was refluxed for 2 h to form a pale-yellow coloured solution. The mixture was cooled to room temperature, after which the solution was allowed to evaporate slowly to obtain crystals of the title salt. ATR-IR (ν_{max}/cm^{-1}): 2923 (N—H stretching of $-NH^{3+}$), 1709 (C═O lactone stretching), 1570 (C═C aromatic ring stretching), 1320 (aromatic C—H stretching). ^{1}H NMR (400 MHz, DMSO-d_6, δ ppm): 4.52 (*s*, 2H, $-CH_2$), 7.51–7.68 (*m*, 7H, Ar—H), 7.75–7.83 (*m*, 4H, Ar—H), 7.96–8.05 (*m*, 1H, Ar—H), 8.84 (*s*, 1H). ^{13}C NMR (100 MHz, DMSO-d_6, δ ppm): 146.6, 143.5, 140.1, 139.4, 138.5, 137.4, 133.9, 131.9, 129.4, 129.2, 128.4, 124.5, 122.5, 120.1, 120.0.

8. Refinement

Crystal data, data collection and structure refinement details are summarized in Table 2. H atoms were positioned with idealized geometry and refined using a riding model with N—H = 0.89 Å and U_{iso}(H) = 1.2U_{eq}(N), and C—H = 0.93 Å for CH groups, 0.97 Å for CH_2 groups and U_{iso}(H) = 1.2U_{eq}(C).

Table 2
Experimental details.

Crystal data	
Chemical formula	$C_7H_{10}N^+\cdot C_{10}H_5O_4^-$
M_r	297.31
Crystal system, space group	Triclinic, $P\overline{1}$
Temperature (K)	296
a, b, c (Å)	6.7505 (5), 7.7881 (6), 14.0809 (10)
α, β, γ (°)	79.644 (2), 84.583 (2), 74.960 (2)
V (Å^3)	702.39 (9)
Z	2
Radiation type	Mo $K\alpha$
μ (mm^{-1})	0.10
Crystal size (mm)	0.27 × 0.24 × 0.22
Data collection	
Diffractometer	Bruker SMART APEXII CCD
Absorption correction	Multi-scan (*SADABS*; Krause et al., 2015)
T_{min}, T_{max}	0.975, 0.979
No. of measured, independent and observed [$I > 2\sigma(I)$] reflections	21216, 3470, 3076
R_{int}	0.043
(sin $\theta/\lambda)_{max}$ (Å^{-1})	0.668
Refinement	
$R[F^2 > 2\sigma(F^2)]$, $wR(F^2)$, S	0.080, 0.161, 1.22
No. of reflections	3470
No. of parameters	200
H-atom treatment	H-atom parameters constrained
$\Delta\rho_{max}$, $\Delta\rho_{min}$ (e Å^{-3})	0.41, −0.38

Computer programs: *APEX2* and *SAINT* (Bruker, 2017), *SHELXT2018/3* (Sheldrick, 2015*a*), *SHELXL2019/2* (Sheldrick, 2015*b*), *Mercury* (Macrae *et al.*, 2020) and *publCIF* (Westrip, 2010).

Acknowledgements

The authors acknowledge the iSTEM, CISEE and are thankful to BSPM's lab for use of their computing facilities. MSK is grateful to the Department of PG Studies and Research in Physics, Albert Einstein Block, UCS, Tumkur University, Tumkur.

References

Ansell, J., Hirsh, J., Hylek, E., Jacobson, A., Crowther, M. & Palareti, G. (2008). *Chest* **133**, 160S-198S.

Atta-ur-Rahman, Choudhary, M. I. & Thomsen, W. J. (2001). *Bioassay Techniques for Drug Development* 1st ed. Newark: CRC press.

Bąkowicz, J., Olejarz, J. & Turowska-Tyrk, I. (2014). *J. Photochem. Photobiol. Chem.* **273**, 34–42.

Bandaru, V., Latambale, G., Kumar, L., Dhuguru, J., Kumari, K. S., Jadhav, V., Juvale, K. & Vidavalur, S. (2025). *Ann. Pharm. Franç.* https://doi.org/10.1016/j.pharma.2025.11.004

Bruker (2017). *APEX2* and *SAINT*. Bruker AXS Inc., Madison, Wisconsin, USA.

Cacabelos, R., Martínez-Iglesias, O., Cacabelos, N., Carrera, I., Corzo, L. & Naidoo, V. (2024). *Life* **14**, 1555.

Chakraborty, P., Das, B., Pal, P., Datta, S., Bera, S. & Dastidar, P. (2020). *Chem. Commun.* **56**, 5251–5254.

Das, U. K., Puranik, V. G. & Dastidar, P. (2012). *Cryst. Growth Des.* **12**, 5864–5868.

Escudero, G. E., Laino, C. H., Echeverría, G. A., Piro, O. E., Martini, N., Rodríguez, A. N., Martínez Medina, J. J., López Tévez, L. L., Ferrer, E. G. & Williams, P. A. (2016). *Chem. Biol. Interact.* **249**, 46–55.

Ganapathi, P., Ganesan, K., Vijaykanth, N., Muthialu, S., Ahmed, S. S., Alam, M. M. & Hussien, M. (2025). *RSC Adv.* **15**, 35115–35136.

Groom, C. R., Bruno, I. J., Lightfoot, M. P. & Ward, S. C. (2016). *Acta Cryst.* B**72**, 171–179.

Hirshfeld, H. L. (1977). *Theor. Chim. Acta* **44**, 129–138.

Ji, H., Tan, Y., Gan, N., Zhang, J., Li, S., Zheng, X., Wang, Z. & Yi, W. (2021). *Bioorg. Med. Chem.* **35**, 115870.

Kemnitzer, W., Drewe, J., Jiang, S., Zhang, H., Wang, Y., Zhao, J., Jia, S., Herich, J., Labreque, D., Storer, R., Meerovitch, K., Bouffard, D., Rej, R., Denis, R., Blais, C., Lamothe, S., Attardo, G., Gourdeau, H., Tseng, B., Kasibhatla, S. & Cai, S. X. (2004). *J. Med. Chem.* **47**, 6299–6310.

Krause, L., Herbst-Irmer, R., Sheldrick, G. M. & Stalke, D. (2015). *J. Appl. Cryst.* **48**, 3–10.

Macrae, C. F., Sovago, I., Cottrell, S. J., Galek, P. T. A., McCabe, P., Pidcock, E., Platings, M., Shields, G. P., Stevens, J. S., Towler, M. & Wood, P. A. (2020). *J. Appl. Cryst.* **53**, 226–235.

Phutdhawong, W., Chuenchid, A., Taechowisan, T., Sirirak, J. & Phutdhawong, W. S. (2021). *Molecules* **26**, 1653.

Pierce, V. M., Bhowmick, T. & Simner, P. J. (2023). *J. Clin. Microbiol.* **61**, e00074–22.

Sheldrick, G. M. (2015*a*). *Acta Cryst.* A**71**, 3–8.

Sheldrick, G. M. (2015*b*). *Acta Cryst.* C**71**, 3–8.

Spackman, M. A. & Jayatilaka, D. (2009). *CrystEngComm* **11**, 19–32.

Spackman, P. R., Turner, M. J., McKinnon, J. J., Wolff, S. K., Grimwood, D. J., Jayatilaka, D. & Spackman, M. A. (2021). *J. Appl. Cryst.* **54**, 1006–1011.

Stefanachi, A., Leonetti, F., Pisani, L., Catto, M. & Carotti, A. (2018). *Molecules* **23**, 250.

Venugopala, K. N., Rashmi, V. & Odhav, B. (2013). *BioMed Res. Int.* 963248.

Westrip, S. P. (2010). *J. Appl. Cryst.* **43**, 920–925.

Yan, D., Delori, A., Lloyd, G. O., Patel, B., Friščić, T., Day, G. M., Bučar, D. K., Jones, W., Lu, J., Wei, M., Evans, D. G. & Duan, X. (2012). *CrystEngComm* **14**, 5121–5123.

Yaşa, M., Celik, E. B., Gao, X. X., Karabağ, Z. G., Gunes, U., Syzgantseva, O. A., Syzgantseva, M. A., Zhong, L., Züttel, A., Dyson, P. J., Nazeeruddin, M. K., Toppare, L., Yerci, S. & Gunbas, G. (2025). *ACS Appl. Mater. Interfaces.* **17**, 18450–18457.

Ye, W., Ma, H., Shi, H., Wang, H., Lv, A., Bian, L., Zhang, M., Ma, C., Ling, K., Gu, M., Mao, Y., Yao, X., Gao, C., Shen, K., Jia, W., Zhi, J., Cai, S., Song, Z., Li, J., Zhang, Y., Lu, S., Liu, K., Dong, C., Wang, Q., Zhou, Y., Yao, W., Zhang, Y., Zhang, H., Zhang, Z., Hang, X., An, Z., Liu, X. & Huang, W. (2021). *Nat. Mater.* **20**, 1539–1544.

supporting information

Acta Cryst. (2026). E**82**, 432-436 [https://doi.org/10.1107/S2056989026003403]

Synthesis, crystal structure and Hirshfeld surface analysis of phenylmethanaminium 2-oxo-2*H*-chromene-3-carboxylate

M. Sunithakumari, M.U. Gagan, V. Dwarakanath, H.T. Srinivasa, H. C. Devarajegowda and B. S. Palakshamurthy

Computing details

Phenylmethanaminium 2-oxo-2*H*-chromene-3-carboxylate

Crystal data

$C_7H_{10}N^+·C_{10}H_5O_4^-$
M_r = 297.31
Triclinic, $P\overline{1}$
Hall symbol: -P 1
a = 6.7505 (5) Å
b = 7.7881 (6) Å
c = 14.0809 (10) Å
α = 79.644 (2)°
β = 84.583 (2)°
γ = 74.960 (2)°
V = 702.39 (9) Å^3
Z = 2
$F(000)$ = 312
co-crystal
D_x = 1.406 Mg m^{-3}
Mo $K\alpha$ radiation, λ = 0.71073 Å
Cell parameters from 3077 reflections
θ = 2–29°
μ = 0.10 mm^{-1}
T = 296 K
Prism, colourless
0.27 × 0.24 × 0.22 mm

Data collection

Bruker SMART APEXII CCD diffractometer
Radiation source: fine-focus sealed tube
Graphite monochromator
Detector resolution: 1.97 pixels mm^{-1}
φ and Ω scans
Absorption correction: multi-scan (SADABS; Krause et al., 2015)
T_{min} = 0.975, T_{max} = 0.979
21216 measured reflections
3470 independent reflections
3076 reflections with $I > 2\sigma(I)$
R_{int} = 0.043
θ_{max} = 28.4°, θ_{min} = 3.0°
h = −8→9
k = −10→10
l = −18→18

Refinement

Refinement on F^2
Least-squares matrix: full
$R[F^2 > 2\sigma(F^2)]$ = 0.080
$wR(F^2)$ = 0.161
S = 1.22
3470 reflections
200 parameters
0 restraints
0 constraints
Primary atom site location: structure-invariant direct methods
Secondary atom site location: difference Fourier map
Hydrogen site location: inferred from neighbouring sites
H-atom parameters constrained
$w = 1/[\sigma^2(F_o^2) + (0.0372P)^2 + 0.9952P]$ where $P = (F_o^2 + 2F_c^2)/3$
$(\Delta/\sigma)_{max}$ < 0.001
$\Delta\rho_{max}$ = 0.41 e Å^{-3}
$\Delta\rho_{min}$ = −0.38 e Å^{-3}

Special details

Geometry. All esds (except the esd in the dihedral angle between two l.s. planes) are estimated using the full covariance matrix. The cell esds are taken into account individually in the estimation of esds in distances, angles and torsion angles; correlations between esds in cell parameters are only used when they are defined by crystal symmetry. An approximate (isotropic) treatment of cell esds is used for estimating esds involving l.s. planes.

Fractional atomic coordinates and isotropic or equivalent isotropic displacement parameters (Å²)

	x	*y*	*z*	U_{iso}*/U_{eq}
O1	0.1596 (2)	0.3659 (2)	0.10082 (12)	0.0219 (4)
O2	−0.0292 (2)	0.4790 (2)	0.22176 (13)	0.0235 (4)
O4	0.4445 (2)	0.5775 (2)	0.33560 (13)	0.0225 (4)
O3	0.2113 (3)	0.4216 (2)	0.39393 (12)	0.0227 (4)
C3	0.3466 (4)	0.3068 (3)	0.05274 (17)	0.0198 (5)
C8	0.5288 (4)	0.3028 (3)	0.09229 (17)	0.0194 (5)
C1	0.3342 (3)	0.4218 (3)	0.23032 (17)	0.0185 (5)
C9	0.5163 (4)	0.3665 (3)	0.18286 (17)	0.0202 (5)
H9	0.636260	0.369672	0.209257	0.024*
N1	−0.2030 (3)	0.4531 (3)	0.43174 (14)	0.0181 (4)
H1A	−0.093073	0.464509	0.393347	0.022*
H1B	−0.216682	0.520552	0.477833	0.022*
H1C	−0.314408	0.489019	0.397146	0.022*
C10	0.3279 (3)	0.4804 (3)	0.32791 (17)	0.0186 (5)
C7	0.7141 (4)	0.2416 (3)	0.04013 (18)	0.0238 (5)
H7	0.838499	0.236871	0.065044	0.029*
C4	0.3414 (4)	0.2571 (3)	−0.03637 (18)	0.0251 (5)
H4	0.217204	0.263651	−0.062042	0.030*
C2	0.1425 (3)	0.4249 (3)	0.18859 (16)	0.0177 (5)
C5	0.5256 (4)	0.1976 (4)	−0.08612 (18)	0.0280 (6)
H5	0.525708	0.163133	−0.146024	0.034*
C12	−0.3402 (4)	0.0714 (3)	0.39657 (19)	0.0278 (6)
H12	−0.460831	0.109011	0.433133	0.033*
C11	−0.1712 (4)	0.1384 (3)	0.40422 (17)	0.0216 (5)
C16	0.0057 (4)	0.0840 (3)	0.34773 (18)	0.0248 (5)
H16	0.118753	0.129561	0.351336	0.030*
C14	−0.1528 (5)	−0.1060 (4)	0.2794 (2)	0.0342 (7)
H14	−0.145768	−0.188100	0.237969	0.041*
C17	−0.1777 (4)	0.2615 (3)	0.47659 (18)	0.0268 (6)
H17A	−0.290682	0.252259	0.523598	0.032*
H17B	−0.051546	0.221327	0.510838	0.032*
C13	−0.3301 (5)	−0.0512 (4)	0.3348 (2)	0.0337 (6)
H13	−0.443188	−0.096414	0.330775	0.040*
C6	0.7118 (4)	0.1886 (4)	−0.04749 (19)	0.0268 (5)
H6	0.834902	0.146506	−0.081327	0.032*
C15	0.0152 (4)	−0.0376 (4)	0.28602 (19)	0.0307 (6)
H15	0.134884	−0.073852	0.248626	0.037*

Atomic displacement parameters (Å²)

	U^{11}	U^{22}	U^{33}	U^{12}	U^{13}	U^{23}
O1	0.0168 (8)	0.0306 (9)	0.0216 (9)	−0.0079 (7)	−0.0042 (6)	−0.0082 (7)
O2	0.0143 (8)	0.0301 (9)	0.0261 (9)	−0.0030 (7)	−0.0025 (7)	−0.0075 (7)
O4	0.0149 (8)	0.0278 (9)	0.0288 (9)	−0.0063 (7)	−0.0049 (7)	−0.0116 (7)
O3	0.0173 (8)	0.0328 (9)	0.0207 (9)	−0.0074 (7)	−0.0012 (6)	−0.0098 (7)
C3	0.0197 (11)	0.0202 (11)	0.0208 (11)	−0.0068 (9)	−0.0022 (9)	−0.0033 (9)
C8	0.0188 (11)	0.0207 (11)	0.0207 (11)	−0.0069 (9)	−0.0033 (9)	−0.0045 (9)
C1	0.0167 (11)	0.0211 (11)	0.0195 (11)	−0.0063 (9)	−0.0048 (9)	−0.0035 (9)
C9	0.0175 (11)	0.0245 (11)	0.0212 (12)	−0.0072 (9)	−0.0060 (9)	−0.0051 (9)
N1	0.0117 (9)	0.0227 (10)	0.0212 (10)	−0.0027 (7)	−0.0044 (7)	−0.0073 (8)
C10	0.0125 (10)	0.0220 (11)	0.0218 (11)	−0.0002 (8)	−0.0066 (8)	−0.0075 (9)
C7	0.0175 (11)	0.0296 (13)	0.0257 (13)	−0.0061 (9)	−0.0019 (9)	−0.0073 (10)
C4	0.0253 (13)	0.0322 (13)	0.0213 (12)	−0.0107 (10)	−0.0061 (10)	−0.0059 (10)
C2	0.0164 (11)	0.0200 (11)	0.0184 (11)	−0.0063 (9)	−0.0039 (8)	−0.0032 (9)
C5	0.0349 (14)	0.0346 (14)	0.0182 (12)	−0.0114 (11)	−0.0009 (10)	−0.0100 (10)
C12	0.0268 (13)	0.0245 (12)	0.0281 (14)	−0.0038 (10)	0.0011 (10)	0.0009 (10)
C11	0.0297 (13)	0.0167 (11)	0.0168 (11)	−0.0023 (9)	−0.0012 (9)	−0.0032 (9)
C16	0.0266 (13)	0.0250 (12)	0.0223 (12)	−0.0047 (10)	−0.0022 (10)	−0.0042 (10)
C14	0.0532 (18)	0.0216 (12)	0.0283 (14)	−0.0036 (12)	−0.0131 (13)	−0.0080 (11)
C17	0.0380 (15)	0.0203 (12)	0.0203 (12)	−0.0020 (10)	−0.0030 (10)	−0.0054 (9)
C13	0.0354 (15)	0.0308 (14)	0.0386 (16)	−0.0138 (12)	−0.0152 (12)	0.0003 (12)
C6	0.0248 (13)	0.0305 (13)	0.0255 (13)	−0.0074 (10)	0.0052 (10)	−0.0082 (10)
C15	0.0340 (15)	0.0288 (13)	0.0236 (13)	0.0043 (11)	−0.0028 (11)	−0.0066 (11)

Geometric parameters (Å, º)

O1—C2	1.379 (3)	C4—C5	1.380 (4)
O1—C3	1.383 (3)	C4—H4	0.9300
O2—C2	1.206 (3)	C5—C6	1.397 (4)
O4—C10	1.249 (3)	C5—H5	0.9300
O3—C10	1.261 (3)	C12—C13	1.387 (4)
C3—C4	1.384 (3)	C12—C11	1.393 (4)
C3—C8	1.389 (3)	C12—H12	0.9300
C8—C7	1.405 (3)	C11—C16	1.385 (4)
C8—C9	1.437 (3)	C11—C17	1.510 (3)
C1—C9	1.348 (3)	C16—C15	1.382 (4)
C1—C2	1.463 (3)	C16—H16	0.9300
C1—C10	1.517 (3)	C14—C13	1.379 (4)
C9—H9	0.9300	C14—C15	1.389 (4)
N1—C17	1.484 (3)	C14—H14	0.9300
N1—H1A	0.8900	C17—H17A	0.9700
N1—H1B	0.8900	C17—H17B	0.9700
N1—H1C	0.8900	C13—H13	0.9300
C7—C6	1.372 (4)	C6—H6	0.9300
C7—H7	0.9300	C15—H15	0.9300

C2—O1—C3	122.79 (17)	O2—C2—C1	126.6 (2)
O1—C3—C4	116.9 (2)	O1—C2—C1	116.8 (2)
O1—C3—C8	120.6 (2)	C4—C5—C6	120.7 (2)
C4—C3—C8	122.5 (2)	C4—C5—H5	119.6
C3—C8—C7	118.1 (2)	C6—C5—H5	119.6
C3—C8—C9	118.0 (2)	C13—C12—C11	120.5 (3)
C7—C8—C9	123.9 (2)	C13—C12—H12	119.8
C9—C1—C2	120.5 (2)	C11—C12—H12	119.8
C9—C1—C10	119.8 (2)	C16—C11—C12	119.0 (2)
C2—C1—C10	119.8 (2)	C16—C11—C17	120.6 (2)
C1—C9—C8	121.3 (2)	C12—C11—C17	120.3 (2)
C1—C9—H9	119.3	C15—C16—C11	120.3 (2)
C8—C9—H9	119.3	C15—C16—H16	119.8
C17—N1—H1A	109.5	C11—C16—H16	119.8
C17—N1—H1B	109.5	C13—C14—C15	119.5 (3)
H1A—N1—H1B	109.5	C13—C14—H14	120.3
C17—N1—H1C	109.5	C15—C14—H14	120.3
H1A—N1—H1C	109.5	N1—C17—C11	113.3 (2)
H1B—N1—H1C	109.5	N1—C17—H17A	108.9
O4—C10—O3	126.4 (2)	C11—C17—H17A	108.9
O4—C10—O3	126.4 (2)	N1—C17—H17B	108.9
O4—C10—C1	116.4 (2)	C11—C17—H17B	108.9
O3—C10—C1	117.1 (2)	H17A—C17—H17B	107.7
O3—C10—C1	117.1 (2)	C14—C13—C12	120.1 (3)
C6—C7—C8	120.1 (2)	C14—C13—H13	119.9
C6—C7—H7	119.9	C12—C13—H13	119.9
C8—C7—H7	119.9	C7—C6—C5	120.3 (2)
C5—C4—C3	118.2 (2)	C7—C6—H6	119.8
C5—C4—H4	120.9	C5—C6—H6	119.8
C3—C4—H4	120.9	C16—C15—C14	120.5 (3)
O2—C2—O1	116.62 (19)	C16—C15—H15	119.7
O2—C2—O1	116.62 (19)	C14—C15—H15	119.7
O2—C2—C1	126.6 (2)		

C2—O1—C3—C4	−177.8 (2)	C3—O1—C2—C1	−0.3 (3)
O1—C3—C8—C7	180.0 (2)	C9—C1—C2—O2	−176.4 (2)
C4—C3—C8—C7	−1.6 (4)	C10—C1—C2—O2	3.9 (4)
O1—C3—C8—C9	−1.7 (3)	C9—C1—C2—O2	−176.4 (2)
C4—C3—C8—C9	176.7 (2)	C10—C1—C2—O2	3.9 (4)
C2—C1—C9—C8	−2.4 (4)	C9—C1—C2—O1	1.2 (3)
C10—C1—C9—C8	177.3 (2)	C10—C1—C2—O1	−178.5 (2)
C3—C8—C9—C1	2.6 (3)	C3—C4—C5—C6	−0.2 (4)
C7—C8—C9—C1	−179.2 (2)	C13—C12—C11—C16	1.4 (4)
C9—C1—C10—O4	42.9 (3)	C13—C12—C11—C17	−175.7 (2)
C2—C1—C10—O4	−137.4 (2)	C12—C11—C16—C15	−1.2 (4)
C9—C1—C10—O3	−134.8 (2)	C17—C11—C16—C15	175.9 (2)
C2—C1—C10—O3	44.9 (3)	C16—C11—C17—N1	78.0 (3)
C9—C1—C10—O3	−134.8 (2)	C12—C11—C17—N1	−104.9 (3)

C2—C1—C10—O3	44.9 (3)	C15—C14—C13—C12	0.0 (4)
C3—C8—C7—C6	0.3 (4)	C11—C12—C13—C14	−0.8 (4)
C9—C8—C7—C6	−177.8 (2)	C8—C7—C6—C5	0.9 (4)
O1—C3—C4—C5	180.0 (2)	C4—C5—C6—C7	−1.0 (4)
C8—C3—C4—C5	1.5 (4)	C11—C16—C15—C14	0.4 (4)
C3—O1—C2—O2	177.5 (2)	C13—C14—C15—C16	0.2 (4)
C3—O1—C2—O2	177.5 (2)		

Hydrogen-bond geometry (Å, º)

*Cg*4 is the centroid of the C11–C16 ring.

D—H···*A*	*D*—H	H···*A*	*D*···*A*	*D*—H···*A*
N1—H1*A*···O2	0.89	2.40	3.068 (3)	132
N1—H1*A*···O3	0.89	1.99	2.752 (3)	142
N1—H1*B*···O3^{i}	0.89	1.94	2.791 (3)	158
N1—H1*C*···O4^{ii}	0.89	1.83	2.716 (3)	174
C17—H17*B*···*Cg*4^{iii}	0.97	2.76	3.613 (3)	147

Symmetry codes: (i) −*x*, −*y*+1, −*z*+1; (ii) *x*−1, *y*, *z*; (iii) −*x*, −*y*, −*z*+1.